



NUMERICAL INVESTIGATION ON THE HYDRODYNAMIC CHARACTERISTICS OF AN AUTONOMOUS UNDERWATER GLIDER WITH DIFFERENT WING LAYOUTS

Muhammad Yasar Javaid¹, Mark Ovinis¹, Nagarajan Thirumalaiswamy¹, Fakhruddin B M Hashim¹, Barkat Ullah¹ and Adi Maimun²

¹Department of Mechanical Engineering, Universiti Teknologi Petronas, Perak, Malaysia

²Marine Technology Centre, Faculty of Mechanical Engineering, Universiti Teknologi Malaysia, Johor Bahru, Malaysia

E-Mail: mark_ovinis@petronas.com.my

ABSTRACT

An autonomous underwater glider is a self-propelled underwater vehicle which is designed primarily for oceanography. It moves with low speed in saw-tooth pattern and has long endurance. The vertical motion of the glider is controlled by changing its buoyancy and its wings convert this vertical motion into horizontal motion. The hydrodynamic coefficients of glider will dictate its performance and possible applications. In this paper, the impact of rectangular and tapered wings on the hydrodynamics coefficient of a glider and the corresponding glide velocity was investigated using ANSYS Computational Fluid Dynamics (CFD) turbulence model and FLUENT flow solver. The lift force of a rectangular wing is higher with less drag force compared to tapered wings. A glider with tapered wings glider will have a larger glide angle and is therefore suitable of deep ocean applications.

Keywords: underwater glider, hydrodynamics and CFD.

INTRODUCTION

An autonomous underwater glider is a special type of autonomous underwater vehicle that have been developed for deep sea exploration. They are attractive because of their high energy efficiency and are capable of longer duration missions and are able to access high-risk areas.

The operating principle of underwater gliders is that at deployment it is negative buoyant and therefore tends to dive, during which its wings convert the downward motion into the horizontal plane, thus producing a forward force. Once a predetermined depth is reached, the vehicle changes its buoyancy to become positively buoyant. This can be done by pumping oil from an internal bladder to an external bladder to the vehicle, thus increasing the vehicle volume but keeping the mass constant [1].

New development efforts have improved the dynamic stability of gliders for deepwater [2] and shallow water [3, 4] operations. Gliders that are in operation or development stage include the Slocum [5], Seaglider [6] and Spray [7]. These gliders are designed for low power consumption and drag force to achieve maximum range and endurance.

Computational fluid dynamics (CFD) is a powerful tool to investigate the hydrodynamic coefficients and pressure distribution around submerged vehicles [8, 9]. Hydrodynamic drag and lift is an important consideration that must be investigated for any underwater vehicle. Hydrodynamic forces are mostly used to define the trajectory of underwater gliders. Wu Jianguo *et al.* [10] investigated the hydrodynamic stability of a hybrid-driven autonomous underwater glider using CFD Fluent. They investigated the rudder, wing and hull of glider separately. CFD was also used to evaluate the stability and manoeuvrability of a hybrid underwater glider with

different wing layouts [11]. The study showed that the lift to drag ratio of a glider wings influences the speed and payload of underwater gliders.

In this paper, the hydrodynamics coefficient of an underwater glider with a fixed wing NACA 0016 profile is investigated using CFD simulation. In addition, the gliding velocity and gliding angles of a glider with rectangular and taper wings of constant wings spans are also investigated. The rectangular shape wing has the capacity to carry large payload due to high lift force with low gliding speed as compared to taper wings.

DYNAMIC MODELING

Graver [1] and Zhang [2] developed the dynamic model of an underwater glider with fixed wings and internal moving masses based on first principles. Let the glider position and orientation in body frame reference be $b = [X_b \ Y_b \ Z_b]$ and $R = [\varphi \ \theta \ \psi]$ respectively. The linear and angular moving velocities of glider are $[V_x \ V_y \ V_z]$ and $[\Omega_x \ \Omega_y \ \Omega_z]$ respectively. The locations of internal masses are shown in Figure-1.

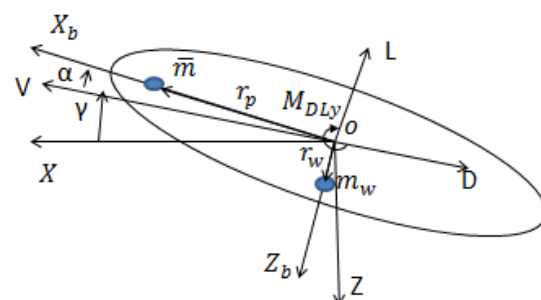


Figure-1. Mass distribution of glider.



The total mass of the glider or body mass can be express as $m_v = m_h + m_w + m_b + m$. m_h is the glider hull mass (uniformly distributed), m_w is point mass with displacement r_w , \bar{m} the movable mass with vector position r_p and m_b is variable ballast mass with respect to geometric centre, GC. The mass 'm' in $m_0 = m_v - m$ is mass of displaced fluid. The glider is neutrally buoyant if m_0 is positive (float) and vice versa.

Dynamic model

Graver [1, 3] simplified the dynamic model of an underwater glider including internal moving masses or ballast mass for stabilization and control of gliders. The equations for the dynamic model can be reduced along the longitudinal plane as given in Equations:

$$v_x = \frac{1}{M_{xd}} [-M_{zd} v_z \Omega_y - m_0 g \sin \theta + L \sin \alpha - D \cos \alpha - u_x] \quad (1)$$

$$v_z = \frac{1}{M_{zd}} [M_{xd} v_x \Omega_y + m_0 g \cos \theta - L \cos \alpha - D \sin \alpha - u_z] \quad (2)$$

$$\dot{\Omega} = \frac{1}{J_y} [(M_{zd} - M_{xd}) v_x v_z - \bar{m} g r_{px} \cos \theta - m_w r_{wz} \sin \theta + M_y - r_{px} u_x] \quad (3)$$

Here, v_x and v_z are components of glider speed V in the longitudinal plane, as shown in Figure 1. ' θ ' is the pitch angle and Ω_y the glider angular velocity. α is angle of attack $\alpha = \left(\frac{v_z}{v_x} \right)$, D and L are the drag and lift of the glider respectively, M_y is the viscous moment, J_y is the inertia element, and u_x and u_z are the total force acting on moveable mass along x and z direction in body fixed.

STEADY STATE

In steady state, the glider stability is a function of the internal mass position with the glider in either a horizontal, upward and downward steady motion. The glide angle and speed of the glider is controlled by varying the position of the internal mass. The control input ballast rate u_b is constant and the simplified dynamics at equilibrium is shown in Figure 2.

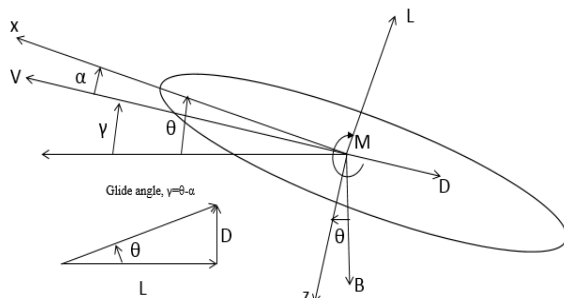


Figure-2. Forces and moments in horizontal plane.

In a steady glide condition, the angular velocity is zero and the translational velocity is constant. The lift force is perpendicular to velocity and the drag force is in an opposite direction to velocity, as shown in Figure-2. These lift, drag and moment forces are dependent on the angle of attack α . The steady gliding motion of an underwater glider is simplified on the XZ plane and the equilibrium gliding angle and speed are given in following equations.

$$0 = -m_0 g \sin \theta + L \sin \alpha - D \cos \alpha \quad (4)$$

$$0 = m_0 g \cos \theta - L \cos \alpha - D \sin \alpha \quad (5)$$

$$0 = -m_w g r_w \sin \theta + M - \bar{m} g r_p \cos \theta \quad (6)$$

HYDRODYNAMIC FORCES

The hydrodynamic forces off an underwater glider is similar to that of aircraft [1, 4]. The hydrodynamics forces are directly related to the angle of attack as given following equations.

$$D = \frac{1}{2} \rho S C_d v^2 = (K_{D0} + K_D \alpha^2) v^2 \quad (7)$$

$$L = \frac{1}{2} \rho S C_L v^2 = (K_{L0} + K_L \alpha) v^2 \quad (8)$$

$$M = \frac{1}{2} \rho S C_M v^2 = (K_{M0} + K_M \alpha) v^2 \quad (9)$$

Here C_D, C_L, C_M are the drag, lift and moment coefficients respectively 'S' characteristic area and ' ρ ' the density of water. The lift and moments forces have a linear relation with the angle of attack ' α ' and the drag force is a quadratic function of α . In above equation K_{D0}, K_D are drag coefficients, K_{L0}, K_L lift coefficients and K_{M0}, K_M moment's coefficients. These coefficients are determined through curve fitting.

METHODOLOGY

In order to determine the hydrodynamic coefficients, fluid is passed over the glider by using CFD Fluent [5, 6]. CFD is a rapidly growing technique for numerical calculation of the hydrodynamic performance of marine vehicles because of its low cost. Most CFD analysis is based on the structure of the fluid and boundary conditions. The fluid structure is dependent on the Reynolds number, which corresponds to a laminar or turbulent flow. The Reynolds number is

$$Re = \rho V L_{glider} / \mu$$

Where L_{glider} is the length of the glider, ρ is water density, V is glider velocity and μ is the viscosity of the fluid. Underwater self-propel vehicles typically have low speeds around 0.25 m/s to 0.5 m/s [7]. Jagadeesh *et al.*



[8] recommended low Reynolds turbulence model for investigation of autonomous underwater vehicles because Reynolds number range between 1×10^5 to 1×10^6 for underwater vehicles. In this work the hydrodynamics of the glider is evaluated through the k- ϵ turbulence model.

COMPUTATIONAL DOMAIN

The fluid domain across the glider is generated based on that recommended in the literature. ITTC [9] recommended that for the fluid domain for surface vehicles, the upstream location should be 1-2 times L_{glider} from the glider and downstream boundary should be 3-5 times L_{glider} to avoid any blockages due to the walls. Similar works on submerged body conclude that the inlet position should be 1.5 times L_{glider} away from the body and the outlet 3.5 times L_{glider} . The top, bottom and side wall should be 9 times D_{glider} to avoid the interruption in fluid flow respectively [6, 7].

In this work, the inlet location of fluid volume is $2L_{glider}$ away from the glider and the outlet location is $6L_{glider}$ from the glider. The wall including ceiling, floor and sides wall is $10D_{glider}$ away from the glider, as shown in Figure-3.

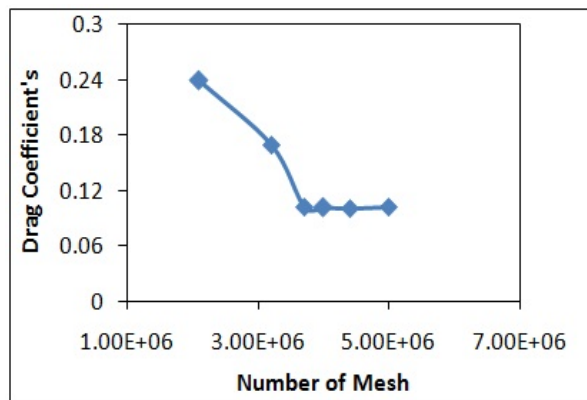


Figure-3. Drag coefficient grid independency numerical simulation.

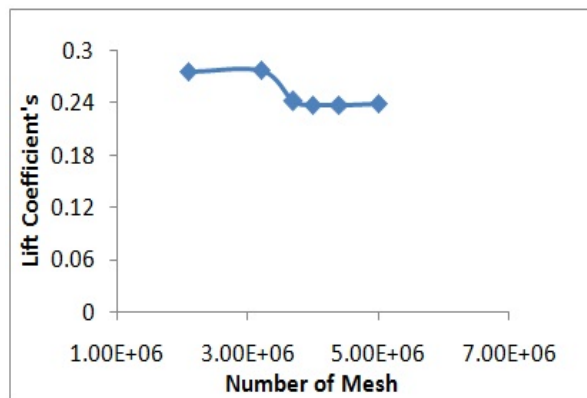


Figure-4. Lift coefficient grid independency numerical simulation.

RESULT AND DISCUSSION

CFD simulation was carried out for an underwater glider with 1.04 m length, 0.28 m diameter with fixed span 0.35 m and chord length 0.17 m of the rectangular and tapered wings respectively as shown in Figure-6. The performance of glider, glide ratio, horizontal velocity and sink rate are directly analogous to the shape of glider wings. Although the payload capacity is depends on the lift force of glider.

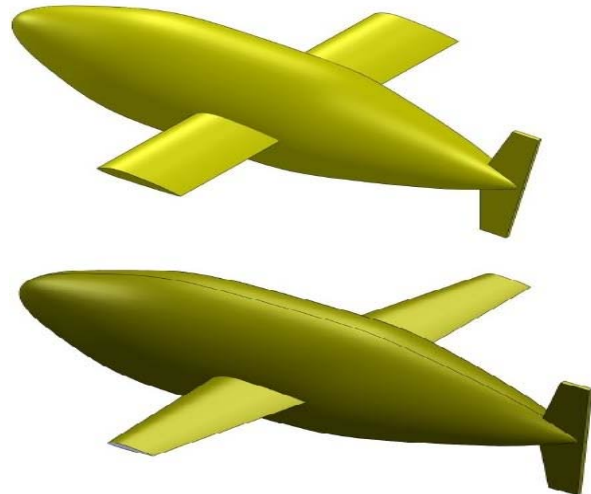


Figure-5. Autonomous underwater glider.

In this study, select two common shapes of wings rectangular and taper because both are used in unmanned marine vehicles. Rectangle wing has a maximum area between leading and trailing edge to create high lift as compared to taper wings. On the other hand, Taper wing has an advantage over rectangular wing in the form of high speed because of less induced drag force. However, the Structural strength of wings are the important factor because of complex hydrodynamic behaviour, taper wing has less strength as compared to rectangular wings and difficult to manufacture.

The hydrodynamic coefficients are investigated at different angles of attack against constant fluid flow and fluid domain. These coefficients are shown in flowing Table-1.

Table-1. Lift and drag coefficients based on CFD simulation.

Coefficients	Taper wing	Rectangular wing
K_{D0}	0.1444	0.1486
K_D	1.975	2.284
K_{L0}	0.08718	0.1087
K_L	3.676	4.196
K_{M0}	-0.09638	-0.07524
K_M	0.8305	0.898



There is considerable increment in lift force of rectangular wing as compare with tapered wing as shown in Figure-6. The increment in lift coefficients of rectangular wing is calculated by equation.

$$\text{Increment (\%)} = \frac{C_{L(\text{Rectangular})}}{C_{L(\text{Tapered})}} - 1 \quad (10)$$

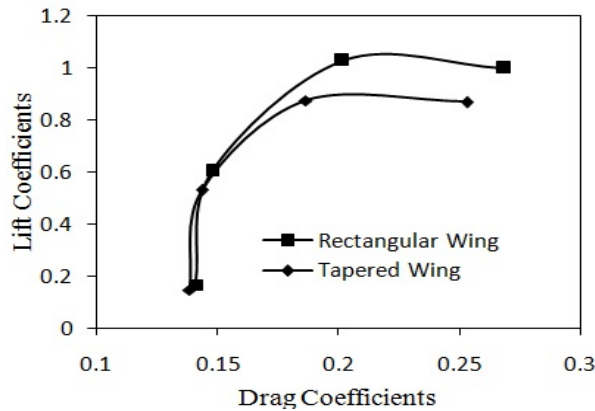


Figure-6. Lift to drag coefficient (lift-drag polar curve).

The lift force is increased by 15% with an increment of 1.8% in drag force for a rectangular wing as compared with a tapered wing with same roots chord length and span. The drag force of a glider is a function of its buoyancy control mechanism, which can be varied by changing the lung capacity factor, as given in Equation.

$$\rho \bar{\eta} V_{vol} \sin \theta = D \quad (11)$$

Here D is the drag force, V_{vol} is the volume of the glider, $\bar{\eta}$ is the lung capacity factor and θ is the glide angle. The lift-to-drag ratio also depends upon the glider wings and the angle of attack. As the angle of attack increases, so does the lift-to-drag ratio. Rectangular wings have 10% more lift-to-drag ratio as compared to tapered wing, as shown in Figure-7.

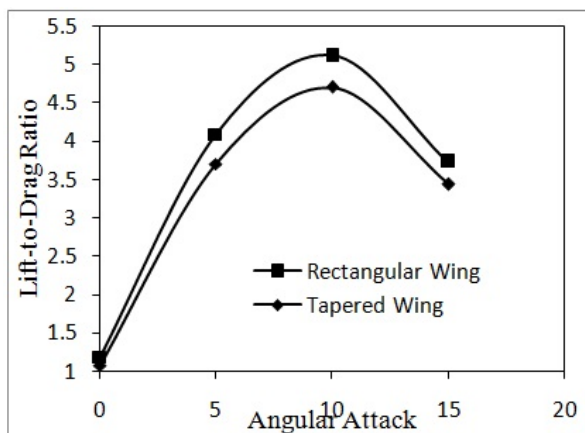


Figure-7. Comparison of lift to drag ratio.

The horizontal and vertical velocity of a glider has a direct relationship to its lift-to-drag ratio. The relationship between lift-to-drag ratios is

$$\frac{L}{D} = \frac{V_x}{V_y} \quad (12)$$

Where V_x is the horizontal velocity and V_y is the vertical velocity. High lift-to-drag ratio is suitable for shallow water applications with high payload capacity and vice versa [10-12].

The velocity and operational range (horizontal speed) of a glider are also a function of its hydrodynamic coefficients. The steady state speed of a glider can be determined from its dynamic equation of the motion. The velocity of glider is given by Equation:

$$V = \sqrt{\frac{2m_0 g \cos \theta}{K_{L0} + K_L \alpha}} \quad (13)$$

Here m_0 is net buoyancy; θ is glide angle and α is angle of attack, which is a function of hydrodynamic forces on the glider. The horizontal velocity of a glider is given by Equation:

$$V_x = V \cos \theta \quad (14)$$

$$V_z = V \sin \theta \quad (15)$$

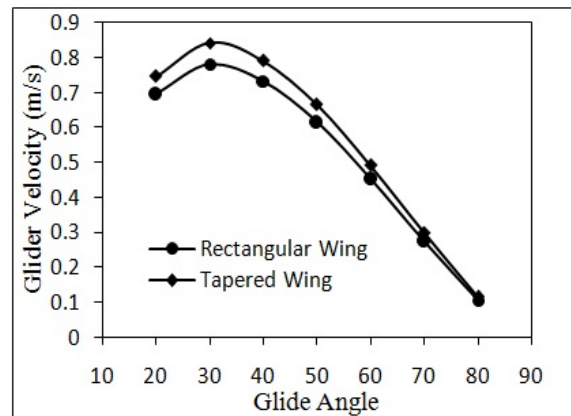


Figure-8. Horizontal velocity at 20 gram net buoyancy.

CONCLUSIONS

The hydrodynamic characteristics of a glider with rectangular and tapered wings have been investigated. Based on a numerical simulation, the rectangular wing geometry produces 15% more lift force with minor increase in drag force with same root chord and spans of wings. Tapered wings, on the other hand, require steeper angle to achieve the maximum glide speed. As such, a glider with rectangular wings will have the capacity to carry a larger payload and is suitable for shallow water applications because of its low glide angle. The results



presented are based on simulation and should be validated experimentally.

ACKNOWLEDGEMENTS

Authors are thankful to Universiti Teknologi Petronas for providing the resources required for this work.

REFERENCES

- [1] J. G. Graver. 2005. Underwater gliders: Dynamics, control and design. Citeseer.
- [2] F. Zhang, J. Thon, C. Thon, and X. Tan. 2012. Miniature underwater glider: Design, modeling, and experimental results in Robotics and Automation (ICRA). IEEE. pp. 4904-4910.
- [3] J. Graver, J. Liu, C. Woolsey, and N. E. Leonard. 1998. Design and analysis of an underwater vehicle for controlled gliding. Proc. 32nd Conference on Information Sciences and Systems. pp. 801-806.
- [4] J. S. Geisbert. 2007. Hydrodynamic modeling for autonomous underwater vehicles using computational and semi-empirical methods. Virginia Polytechnic Institute and State University.
- [5] F. I. Fluent 6.1 User's Guide.
- [6] O. M. J. M. Yasar, T. Nagarajan, S. S. A. Ali and U. Barkat. 2015. Study on Wing Aspect Ratio on the Performance of a Gliding Robotic Fish. Applied Mechanics and Materials, vol. 789(2015). pp. 248-253.
- [7] S. Zhang, J. Yu, A. Zhang and F. Zhang. 2013. Spiraling motion of underwater gliders: Modeling, analysis, and experimental results. Ocean Engineering, vol. 60. pp. 1-13.
- [8] P. Jagadeesh, K. Murali and V. Idichandy. 2009. Experimental investigation of hydrodynamic force coefficients over AUV hull form. Ocean Engineering, vol. 36. pp. 113-118.
- [9] V. Bertram. 2011. Practical ship hydrodynamics: Elsevier.
- [10] M. Y. Javaid, M. Ovinis, T. Nagarajan and F. B. Hashim. 2014. Underwater Gliders: A Review. MATEC Web of Conferences. p. 02020.
- [11] M. F. Ibrahim, M. Ovinis and K. Shehabuddeen. 2013. An Underwater Glider for Subsea Intervention: A Technical Feasibility Study. Applied Mechanics and Materials, vol. 393. pp. 561-566.
- [12] S. A. Jenkins, D. E. Humphreys, J. Sherman, J. O. C. Jones and N. Leonard. 2003. Underwater glider system study.